Journal of Engineering Physics and Thermophysics, Vol. 79, No. 4, 2006

INTERACTION OF A COMBINATION OF BODIES IN SUPERSONIC FLOW. INTERFERENCE AND DIFFRACTION OF SHOCK WAVES IN FLOW OVER TWO BODIES OF REVOLUTION

V. F. Volkov and E. K. Derunov

UDC 533.601 + 629.135

Results are presented of numerical investigations of three-dimensional supersonic flows in a disturbed region of jointly streamlined two identical bodies arranged in parallel which represent combinations of a cone with a semivertex angle of 20° and a cylinder with a fineness ratio of 5. Longitudinal flow over bodies has been studied numerically based on the Euler equation at a Mach number of incident flow equal to 4.03 and a zero angle of attack. The effect has been shown of the distance between the axes of models on the flow structure and disturbed and total aerodynamic characteristics of bodies. Calculated results have been compared with data of the physical experiment.

When two bodies are simultaneously exposed to supersonic flow, an intricate flow picture is observed, which mainly manifests itself in the space between bodies, namely, in the intermodel space. In the vicinity of bodies occur the interaction of shock waves with rarefaction waves, interference and refraction of shock waves, the formation of secondary shocks, and reflection and diffraction of waves on the surface of the bodies. All these phenomena are accompanied by the origination, on the surface of bodies, of various-length regions of high and low pressures, which in turn leads to a change in aerodynamic characteristics.

Supersonic interference of flow over a combination of bodies was considered in [1–8]. Thus, in experimental studies [1, 2] with symmetrical flow over two identical bodies of revolution analysis is made of the effect of the determining parameters, such as the Mach number of incident flow and the distance between bodies, on loads disturbed over the surface of bodies and their total aerodynamic characteristics.

The effect of the Mach numbers and angle of attack on total loads of a body of revolution in its supersonic interaction with a flat surface was dealt with in study [3].

Results of numerical calculations of supersonic interference are presented in [4], where consideration was given to the problems of flow over a single body of revolution near a plane and a slightly curved surface, and the effect of the curvature of a closely adjacent surface on gasdynamic parameters disturbed over the body surface.

A comparison of the calculated results and experimental data for loads disturbed over the surface of bodies and for total aerodynamic characteristics with supersonic flow over a combination of two bodies of revolution is given in [5]. It is shown that when use is made of the algorithm based on a stationary analog of Godunov's difference scheme, the maximum discrepancy between the experimental and calculated results is observed in the region of separation where a conic front shock interacts with a turbulent boundary layer of the model.

Experimental investigations of the interaction of one or two bodies of revolution above a flat surface (a plate) are presented respectively in [6, 7], where the emphasis was on the pressure distribution on the models.

Among the problems of the supersonic interaction of a group of bodies is that examined in [8]. Consideration was given to the process of separation of the stages of carrier rockets arranged according to a longitudinal scheme. Disturbed loads on the rocket stages and their aerodynamic characteristics were calculated for Mach numbers $M_\infty = 4$ and different angles of attack.

Institute of Theoretical and Applied Mechanics, Siberian Branch of the Russian Academy of Sciences, 4/1 Institutskaya Str., Novosibirsk, 630090, Russia; email: volkov@itam.nsc.ru. Translated from Inzhenerno-Fizicheskii Zhurnal, Vol. 79, No. 4, pp. 81–90, July–August, 2006. Original article submitted December 3, 2004; revision submitted August 5, 2005.

1062-0125/06/7904-0712 ©2006 Springer Science+Business Media, Inc.

The numerical scheme used in the current work was verified in [9], where results are given of calculating three-dimensional supersonic flows at $M_\infty = 4.03$ in the vicinity of two identical bodies of revolution positioned above a plate at a zero angle of attack. The bodies represented combinations of a core with the semivertex angles $\theta = 20^o$ (and 30^o) with a cylinder with the diameter D and the fineness ratio $\lambda_c = 5$. The results, obtained for the distance of the bodies from the plate $\Delta y = 0.96D$ and various distances Δz between the bodies, were compared with numerical calculations [7] and data of the physical experiment [2] on the gasdynamic structure, pressure distribution, and limiting streamlines on the surfaces of the bodies and plate.

Notwithstanding the diversity of the studies made, the prediction of a wave structure in the disturbed region and of aerodynamic characteristics with account for the effect of the characteristic parameters remains a topical problem. The increased capabilities of computer engineering for carrying out numerical calculations followed by processing of the results allow a more detailed investigation of the effect of the determining parameters on the formation of a wave structure of flow in the disturbed region when a group of bodies is simultaneously immersed in longitudinal flow. The objective of this study is numerical calculation of the supersonic interaction of two axisymmetric bodies arranged in parallel. The effect of the distance Δz between bodies on the gasdynamic structure of flow in the disturbed region, loads disturbed over the surface of bodies, and their total aerodynamic characteristics is examined.

Formulation of the Problem. Consideration is given to supersonic flow of a viscous compressible gas over two identical bodies of evolution. The solution is sought in a Cartesian system of coordinates xyz in the region bounded by the surface of a body, the bow wave, and the plane of symmetry between the bodies.

The equations of unsteady motion of a compressible gas under the condition of absence of sources and drains for a certain finite volume inside the disturbed region are of the form [10, 11]

$$\iiint\limits_{\Omega} \frac{\partial f}{\partial t}\, d\Omega + \iint\limits_{S} \mathbf{F}\,(g)\, d\mathbf{S} = 0\,.$$

The region of solution is broken up into finite nonoverlapping volumes. Initial equations are approximated on each elementary volume, and the values of gasdynamic parameters on the cell faces are redetermined linearly form their magnitudes at nodal points.

A steady solution of the problem of flow over a body with a specified initial flow field is found using the time-dependent technique in each section x = const. Here, the flow parameters in the first Marsh section are calculated on the condition that flow in the vicinity of the tip of a body is conical. As the solution is established, the position of the bow wave is corrected.

Boundary conditions are as follows: the condition of nonleak on the surfaces of a body and a plate, the condition of flow symmetry with respect to the plane between bodies; on the surface of the shock wave; flow parameters in the disturbed region are connected with parameters of the incident flow by the Rankine–Hugoniot relations; the condition of "splicing" of the solutions over the circumferential coordinate is accomplished on the plane $x0y$ corresponding to $\varphi = 0$.

The employed numerical algorithm provides the calculation with an isolation of the bow wave during the solution of the problem as well as using the through method. In the first case, the solution is carried out on an adapting grid, which follows the position of the bow wave and is determined on each iteration time step. In the second case, the calculation is performed on a fixed grid, and parameters of the incident flow are specified on the external boundary. The preliminary stage in the solution of the problem of supersonic interaction of two bodies is the solution of the problem of flow over an equivalent isolated body of revolution. At this stage, flow parameters in the disturbed region are determined and the position of the external boundary of the calculation region is refined. Results of the solution of this problem are used as the initial data for solving the main problem.

Calculated Results. The character and structure of flow in the vicinity of bodies depend on the Mach number of the incident flow M_∞, geometry of bodies, and distance between them Δz. It should be noted that at the preliminary stage the supposed structure of shock waves in the intermodel channel can be assessed using the laws of reflection of geometric optics. In this case, the interaction of front shocks with the angle of inclination β begins near the section $x_1 = \Delta z/(2 \tan \beta)$, and the first reflection and appearance of the region of elevated pressure on the surface of closely spaced bodies are possible at $x_2 = x_1 + (\Delta z - D)/(2 \tan \beta)$. In accordance with this assessment, in the sections x_k =

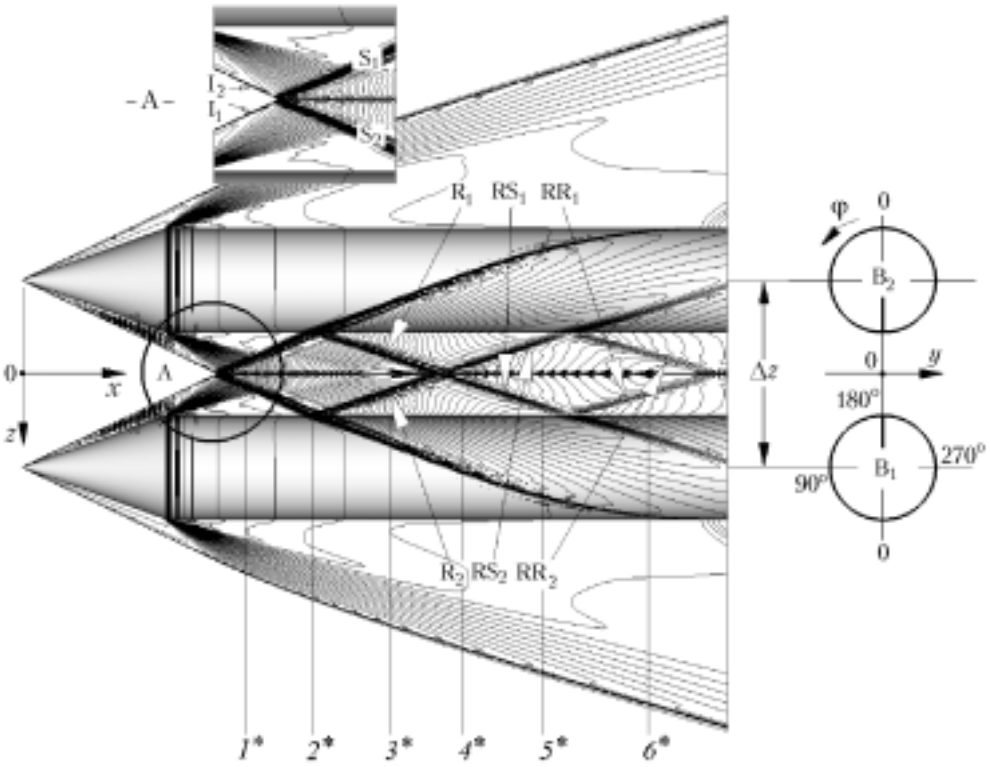

Fig. 1. Wave structure of flow in the vicinity of interacting bodies at M_∞ = 4.03, $\theta = 20^o$, and $\Delta z = 1.8D$.

$x_1 + (k-1)\Delta x$ with the step $\Delta x = (\Delta z - D)/\tan\beta$ in the intermodel space in sections $x_k = x_1(k-1)\Delta x$ a periodic interaction of shock wave is realized, and their reflection and diffraction set up the prerequisite for a periodic appearance of the regions of elevated pressure on the surface of a body. The multiplicity of the series k of interacting and reflected shocks is determined from the condition $x_k \le L$, and at $k = [(2L \tan\beta - \Delta z)/(\Delta z - D)] < 1$ the flow picture in the vicinity of bodies corresponds to flow over a single body. We conventionally call the integral part of the quantity k the interaction multiplicity. This assessment disregards the refraction of shock waves and the types of their interaction and still, in the first approximation, gives an opportunity for evaluating the effect of the distance between bodies Δz on the supposed flow structure in the disturbed region. At a fixed value of the Mach number of the incident flow (β = const), the wave structure and flow character in the disturbed region are mainly determined by the distance between bodies Δz.

We solve the problem of longitudinal flow over two identical axisymmetric bodies at zero angle of attack, whose axes are parallel and belong to the plane $x0z$. The body of revolution represents a combination of a cone with a semivertex angle of 20^o and a cylinder with the fineness ratio $\lambda_c = (L - x_h)/D = 5$. The spacing of bodies is determined by the distance Δz between their axes. The plane $x0y$ ($\Delta z/2$) is the plane of symmetry for two bodies (Fig. 1). For the presented scheme, flow in the disturbed region is symmetric with respect to the plane $x0y$, and in this case the problem is equivalent to the problem of flow over a single body in the presence of a plane.

A more detailed flow picture in the vicinity and on the surface of two bodies is afforded by the results of solving the problem of joint streamlining of bodies at M_∞ = 4.03 and $\Delta z = 1.8D$.

A complete picture of the distribution of gasdynamic parameters over the surface of bodies and of their spatial wave structure can be obtained by examining Figs. 1 and 2 together. Figure 1 shows the wave structure of flow and the distributions of density (ρ) isolines over the surface of the main (B_1) and auxiliary (B_2) bodies and in the plane $x0z$ of the disturbed space, whereas Fig. 2 demonstrates the distribution of density isolines in the cross section of the vicinity of the model B_2, where the numbers of sections and their coordinates correspond to the sections indicated in Fig. 1.

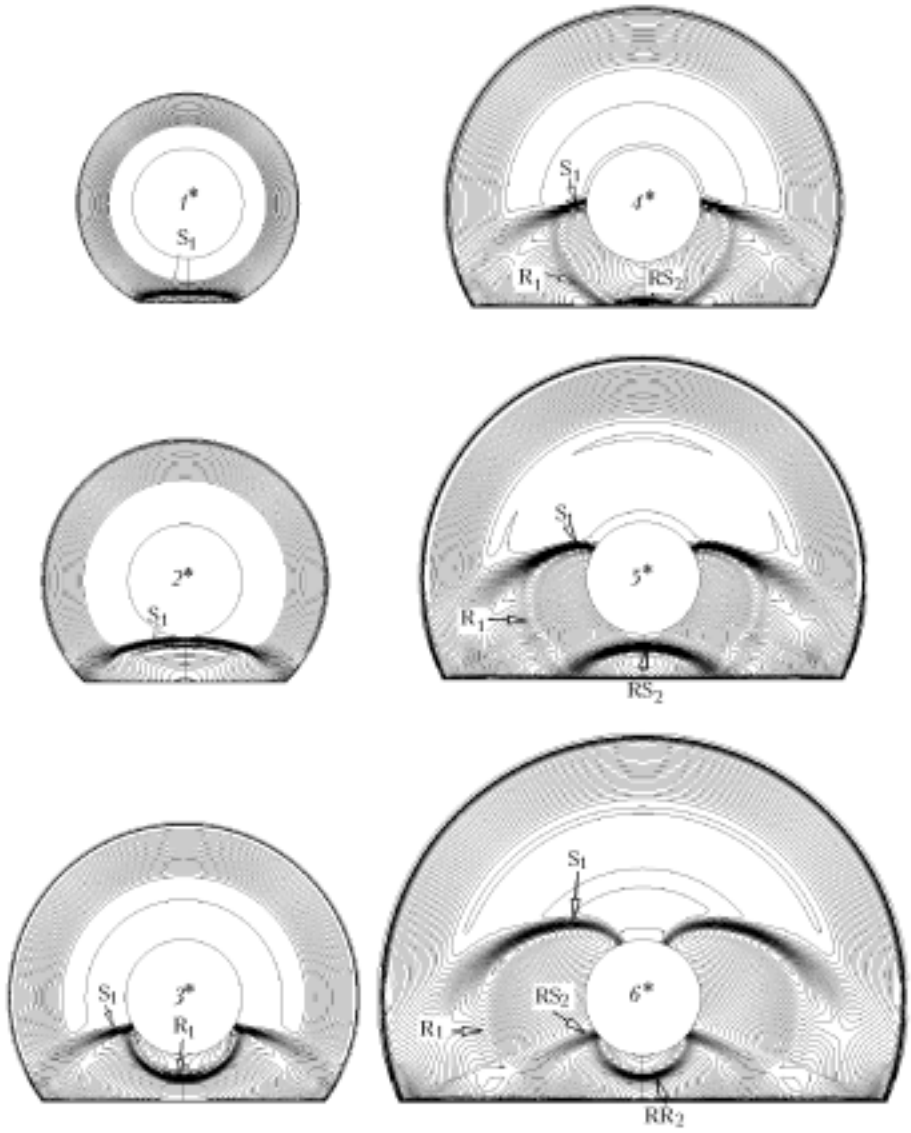

Fig. 2. Wave structure of flow in cross sections 1^*–6^* at $M_\infty = 4.03$, $\theta = 20^o$, and $\Delta z = 1.8D$: 1^*, $x = 2.12D$; 2^*, $2.76D$; 3^*, $3.5D$; 4^*, $4.2D$; 5^*, $4.95D$; and 6^*, $5.97D$.

With specified geometry of bodies and flow conditions bow waves are attached to the nose of the cone. In the section where the head adjoins the cylinder, an axisymmetric centered rarefaction wave is realized. The "opposing" interaction of the axisymmetric bow waves I_1 and I_2 respectively from the main and auxiliary modes (see the boxed-off enlarged fragment A in Fig. 1) occurs along the line of their intersection with the vertex in the section $x_1 = \Delta z/(2 \tan \beta)$ on the plane $x0z$. At the specified value $\Delta z = 1.8D$, the vertex of the line of intersection of bow waves in the plane $x0z$ lies in the region of the influence of rarefaction waves, which leads to a decrease in their intensity and angle of attack. The intensity and the angle of "encounter" $\omega \approx 2\beta < \omega_{cr}$ of the front shocks I_1 and I_2 corresponds to the mode of normal regular interaction [12, 13].

The interaction of the front shocks I_1 and I_2 on the line of their intersection results in the formation of the outgoing waves S_1 and S_2, respectively. The wave structure in the plane $x0z$ with corresponding designation of waves is shown in Fig. 1 and incorporates the propagation of outgoing waves, the interaction of shock waves in the disturbed region, and the reflection and diffraction of shocks on the surface of bodies.

The sequence of formation of the shock-wave picture in the longitudinal direction of the intermodel channel can conventionally be defined by the chains (Figs. 1, 2)

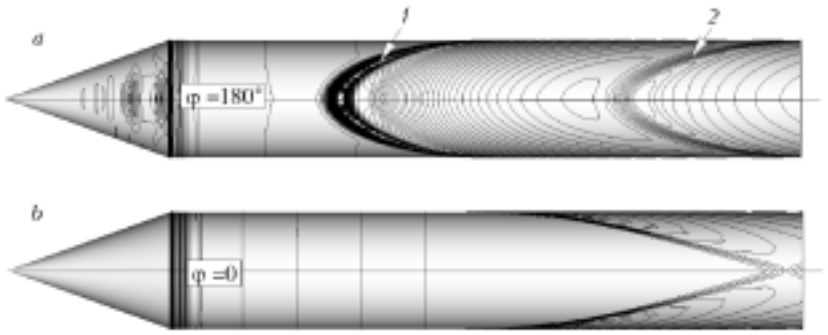

Fig. 3. Distribution of density isolines over the surfaces BS_1 (a) and BS_2 (b) at $M_\infty = 4.03$, $\theta = 20^o$, and $\Delta z = 1.8D$: 1 and 2, tracks of shock waves.

$$I_1 \rightarrow S_1 \rightarrow B_2 \rightarrow R_1 \rightarrow RS_1 \rightarrow B_1 \rightarrow RR_1 \rightarrow B_2 , \quad (1)$$

$$I_2 \rightarrow S_2 \rightarrow B_1 \rightarrow R_2 \rightarrow RS_2 \rightarrow B_2 \rightarrow RR_2 \rightarrow B_1 . \quad (2)$$

Here, I stands for bow waves, S for outgoing waves, B for models, R for primary reflected waves S, RS for outgoing waves with an "opposing" interaction of the primary reflected waves R, and RR for secondary reflected waves. Subscripts 1 and 2 denote the sequence of the wave propagation, and the arrow indicates its direction. Since the wave structure is symmetric with respect to the plane $x0y$, it is sufficient to trace dynamics of the propagation of an outgoing wave relying on one of the chains.

The interaction of bow and outgoing shock waves with centered rarefaction waves is shown on the fragment A in Fig. 1. Here, the outgoing waves S_1 and S_2 propagate downstream respectively in the direction of the models B_2 ($S_1 \rightarrow B_2$) and B_1 ($S_2 \rightarrow B_1$), reflect from them, and interact with one another on the plane of symmetry $x0y$. The outgoing wave S_1 related to the model B_2 is an incident wave. In this case, both reflection ($S_1 \rightarrow B_2 \rightarrow R_1$) and diffraction of the wave S_1 can take place on the body surface. Reflection with the formation of the shock R_1 occurs on the body surface BS_1 and is realized provided $\delta = \arccos [\mathbf{wn}(\varphi)] < 0$. The diffraction phenomenon is possible with angles $\delta > 0$ [12, 13], i.e., shock waves propagate to the region of the surface BS_2. Here, δ is the angle between the velocity vector **w** behind the incident wave S_1 and the body surface; BS_1 is inside surfaces of the bodies B_1 and B_2 in the angle interval $90^o < \varphi < 270^o$, which face one another; and BS_2 is outside surfaces in the angle interval $90^o > \varphi > 270^o$, which are opposite to them.

For the considered flow regime, on the surface BS_1 of the model B_2 cylinder a regular reflection of the wave S_1 proceeds along line 1 having the shape of hyperbola (Fig. 3a) with the vertex on the generatrix $\varphi = 180^o$. Here, the first horseshoe-shaped region of elevated pressure is formed on the surface of bodies behind the reflected wave R_1. The propagation of the reflected shock R_1 to the model B_1 ($R_1 \rightarrow B_1$) is demonstrated in Fig. 1 and in sections 3^* and 4^* in Fig. 2. A regular secondary interaction of waves in the disturbed region occurs when the reflected shocks R_1 and R_2 intersect on the plane $x0y$. Downstream, the outgoing waves RS_1 and RS_2 propagate correspondingly in the direction to the bodies B_1 and B_2 (Fig. 2, section 5^*). The second region of flow reduction on the surface BS_1 (Fig. 3a) is formed along line 2 under the effect of the reflected wave RS_2. The reflected shock RR_2 in turn results from the secondary reflection of the outgoing wave S_2 (Figs. 1 and 2, section 6^*).

As stated above, the propagation of shock waves in the disturbed region under the condition $\delta > 0$ is accompanied by diffraction on the surface of bodies. The diffraction phenomenon is manifested when the outgoing shock waves S_1 and S_2 propagate to the intermodel space. The sequence of the passage around the surface B_2 by the shock wave S_1 as it propagates to the region of the surface BS_2 is shown in Fig. 2 (sections 3^*–6^*). The track of diffracted waves on the surface BS_2 of the body B_2 is indicated in Fig. 3b. It can also be seen here that diffracted waves interact at the back of the body near the generatrix $\varphi = 0$.

The loads, distributed over the surfaces of bodies in transverse and longitudinal directions, are presented in Figs. 4 and 5, respectively. It should be noted that, in Fig. 4, the distribution of the coefficients $C_p(\varphi)$ in the interval

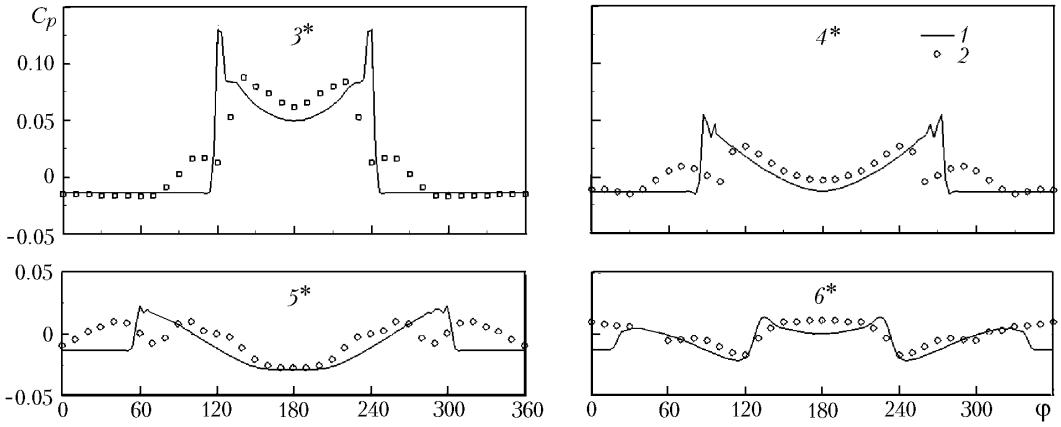

Fig. 4. Distribution of pressure coefficients over cross sections of a body at $\Delta z = 1.8D$ (1, calculation; and 2, experiment): 3^*, $3.5D$; 4^*, $4.2D$; 5^*, $4.95D$; and 6^*, $5.97D$.

$90^o < \varphi < 270^o$ refers to the surface BS_1, and in the interval $90^o > \varphi > 270^o$, to the surface BS_2. The first horseshoe-shaped region of elevated pressure on the surface BS_1 is visible in the sections $x = 3.5D$ and $x = 4.2D$. Here, peaks of $C_p(\varphi)$ correspond to the strength of the shock R_1 on the line of reflection with a decreasing amplitude, according to the condition $\delta < 0$. The maximum strength of the reflected shock is realized at the vertex $x_1 = \Delta z/(2 \tan \beta)$ of the line of reflection.

The pressure size accompanying the diffraction of waves on the surface BS_2 is demonstrated by the $C_p(\varphi)$ distribution in the sections $x = 4.95D$ and $x = 5.97D$. It should be noted that in the section $x = 4.95D$ the increased value of $C_p(\varphi)$ in the interval $90^o < \varphi < 270^o$ results from the secondary reflection and refers to the second horseshoe-shaped region on the surface BS_1 (Fig. 3a). The comparison of calculated results with experimental data presented in Fig. 4 indicates their qualitative agreement. The differences observed near the lines of reflection and diffraction of shock waves on the body surface are attributed to the effect of the separation of the boundary layer or at least to secondary flows originating in it [8], which are not described within the framework of the employed model of a nonviscous gas.

In Fig. 5, curves of the $C_p(x)$ distribution for the considered variant $\Delta z = 1.8D$ are labeled 2. It is possible to distinguish the following trends in the variation of the coefficients C_p on the body surface in the longitudinal direction. On the generatrix $\varphi = 180^o$, the dependence $C_p(x)$ is a periodic sawtooth function with a decreasing amplitude in character. Here, the second peak of the values of C_p corresponds to the strength of the secondary reflected shock RR_2 (Fig. 1). Its sharp decrease results from the effect of an axisymmetric rarefaction wave on intermediate shock waves in the intermodel space. On the lateral generatrices $\varphi = 90^o$ (270^o) diffraction of the outgoing wave S_1 leads to a decrease in the amplitude of the peak of the coefficient C_p, and the monotonically decreasing form of the function $C_p(x)$ is due to the wave RS_2 leaveing the body surface. The interaction of diffracted waves near the surface BS_2 (Fig. 3b) manifests itself in a pressure rise on the generatrix $\varphi = 0$ (Fig. 5, curve 2) at the front of the body $x \approx 6.5D$.

It should be noted that the first region of elevated pressure on the surface BS_1 of the main model is formed as a result of the effect of a bow wave of the closely adjacent auxiliary model. The presence of the second region of elevated pressure is attributed to the effect of its own bow wave reflected from the auxiliary model.

As estimates showed, for the considered geometry of bodies at a fixed Mach number of the incident flow the basic parameter affecting the wave structure and flow pattern in the disturbed region is the distance Δz. It has an appreciable effect on the variation in the step Δx of periodicity of origination of interacting shock waves in the disturbed region and of those reflected on the body surface, i.e., leads to a change in the interaction multiplicity k. Evidently, a variation in the distance Δz causes a displacement of the points of intersection of the front shocks $x_1 = \Delta z/(2 \tan \beta)$ and a corresponding shift of horseshoe-shaped regions on the body surface BS_1. Thus, with increasing distance the beginning of the opposing interaction of bow waves shifts toward the nose of the body and is outside the region of influence of a centered rarefaction wave, which leads to a corresponding displacement of the entire wave structure and a sharp increase in the amplitude of the first reflected wave. A multiple interaction of shocks is realized in the dis-

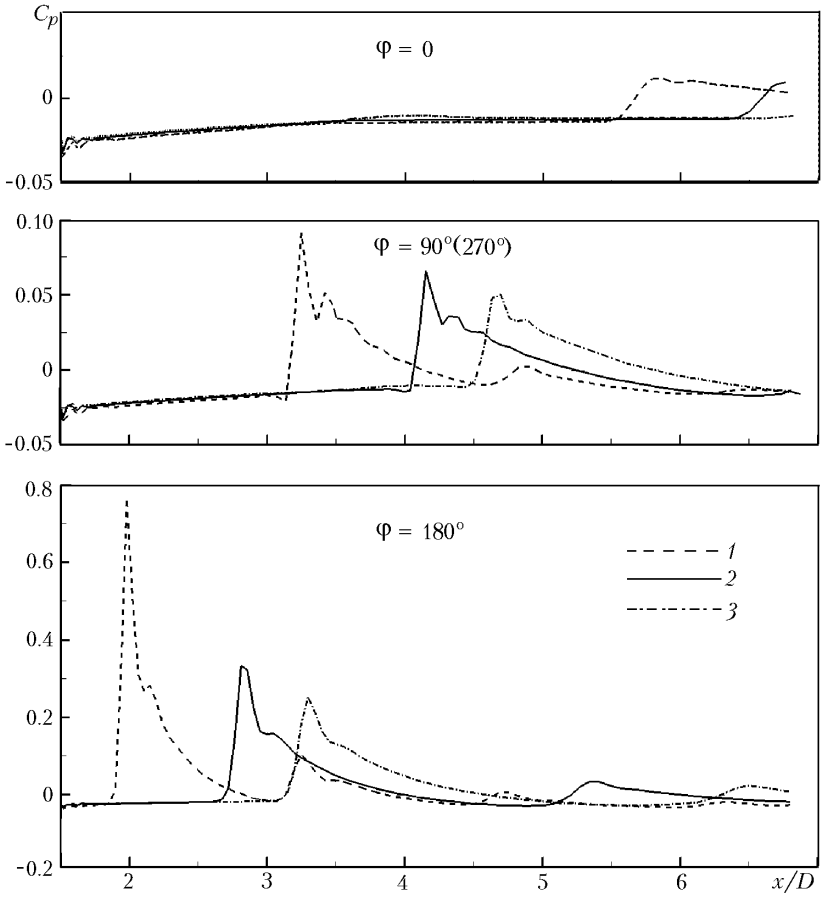

Fig. 5. Distribution of pressure coefficients over generatrices of the body surface at $M_\infty = 4.03$, and $\theta = 20^o$: 1, $\Delta z = 1.4D$; 2, $1.8D$; and 3, $2.0D$.

turbed region, and horseshoe-shaped regions of elevated pressure appear on the body surface BS_1. In turn, a decrease in the periodicity step Δx leads to an increase in the amplitude of reflected waves, to a diminishing of the size of horseshoe-shaped regions on the surface BS_1 in the longitudinal direction, and to a growing influence of the wave diffraction on the load distribution over the surface of bodies. For example, at $\Delta z = 1.4D$ along the generatrix $\varphi = 180^o$ the $C_p(x)$ distribution (Fig. 5, curve 1) takes the form of a periodic function, whose local maxima correspond to the strength of reflected waves with amplitude decreasing as they propagate downstream. At the same time, the flowing influence of the wave diffraction on local loads is illustrated by curve 1 (Fig. 5) along the generatrix $\varphi = 0$. Here, in comparison with the variant $\Delta z = 1.8D$, the region of pressure rise is markedly extended and the degree of flow reduction is increased.

The pattern of the effect of the distance Δz on the variation of the distribution of gasdynamic parameters over the body surface is shown by an example of joint streamlining of bodies at $\Delta z = 1.2D$. A series of reflected waves is illustrated by the distribution of density isolines over the surface BS_1 in Fig. 6a. In Fig. 6b the effect of the wave diffraction on parameters distributed over the surface BS_2 manifests itself much sooner than with the variant $\Delta z = 1.8D$. The $C_p(\varphi)$ distribution near the front of the body is shown in Fig. 6c where increased values of the pressure coefficients in the interval $90^o > \varphi > 270^o$ are realized due to diffraction of shock waves with their propagation to the surface BS_2.

When the distance increases to $\Delta z = 2D$, the vertex of the line of intersection of front shocks falls within the region of influence of centered rarefaction waves. The displacement of the line of opposing interaction of bow waves leads to a corresponding displacement of horseshoe-shaped regions. On the body surface BS_1 at $\Delta z = 2D$ double reflection of outgoing waves is realized with the formation of two horseshoe-shaped regions. Secondary reflection occurs at the front of the body at $x \approx 6.5D$. The growing influence of strong rarefaction waves leads to a marked decrease

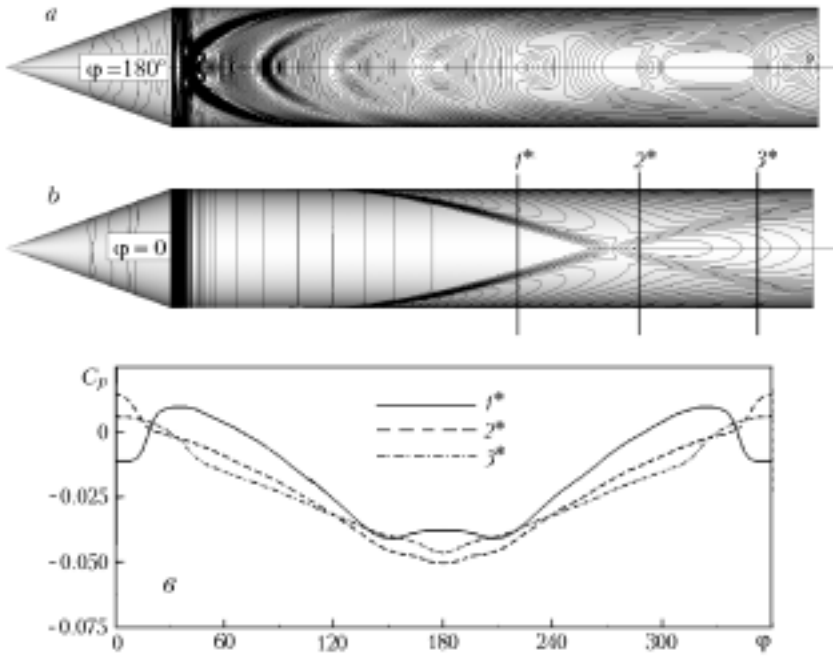

Fig. 6. Distribution of density over the body surface and of pressure coefficients over the cross sections at $\Delta z = 1.2D$ (1^*, $x = 4.5D$; 2^*, $5.47D$; and 3^*, $6.5D$): a, over the surface BS_1; b, over the surface BS_2; and c, over various cross sections.

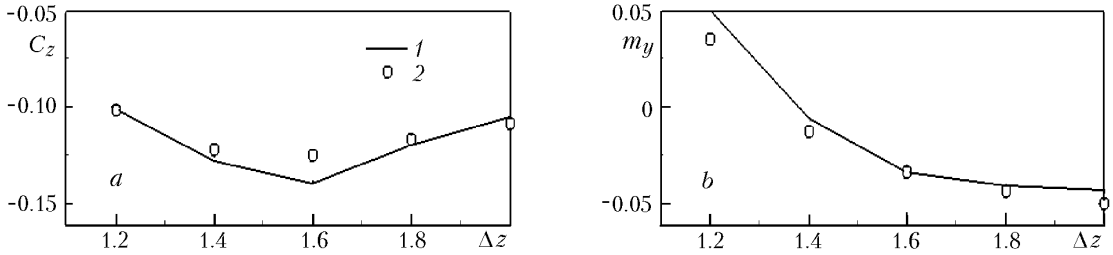

Fig. 7. Aerodynamic characteristics as functions of the distance between bodies (1, calculation; and 2, experiment): a, coefficients of repulsive force; and b, coefficient of yaw moment).

in the strength of intersecting and outgoing shock waves, which in turn causes a decrease in the strength of the first reflected wave. Secondary reflection manifests itself in the presence of the second peak in the $C_p(x)$ distribution (Fig. 5, curve 3) along the generatrix $\varphi = 180^o$. Here it should be noted that, in the vicinity of the body surface BS_2, the interaction of diffracted waves does not occur and the $C_p(x)$ distribution on the generatrix $\varphi = 0$ corresponds to flow over an isolated body.

Thus, with increase in the distance Δz between bodies the effect of centered rarefaction waves on the strength of bow waves becomes larger. In the disturbed region, the wave structure shifts downstream and the amplitude of reflected shocks decreases. The period of appearance of reflected waves on the surface of bodies increases, leading to the extension of horseshoe-shaped regions of elevated pressure on the surface BS_1 of bodies. Furthermore, the effect of diffracted waves on loads distributed over the body surface diminishes.

The predominant factor of the effect of a closely adjacent body is the formation of the first horseshoe-shaped region of flow reduction on the surface BS_1 of the main model. It is precisely the degree of flow reduction in this region and its size and location that will determine the overall aerodynamic characteristics arising in the joint supersonic flight of two bodies.

Figure 7 presents relations for the coefficients of lateral forces C_z and yaw momenta m_y in the distance range $\Delta z = 1.2D - 2D$. The aerodynamic coefficients were calculated taking the diameter of the cylindrical part D and the body length L as characteristic dimensions. Here pertinent experimental data are also presented. It should be noted that, in the Δz range considered, only repulsive forces act on the bodies. In this case, the variation in the coefficient C_z with the distance is of nonlinear character with a minimum in the vicinity of $\Delta z = 1.6D$. This is explained by the fact that with short distances ($\Delta z = 1.2D$) the predominant effect on local loads is exerted by an increase in the strength of reflected waves and their multiplicity on the body surface (Fig. 6a). With the distance $\Delta z = 2D$, the decrease in the amplitude of reflected shocks is compensated by an enlargement of the region of pressure rise on the body surface BS_1 in the longitudinal direction.

Variations in the coefficients of yaw momenta m_y with the distance Δz are shown in Fig. 7b. Here, the point of reduction of moments is located in the nose of a body. In the range of the distances Δz considered, the dependence $m_y(\Delta z)$ is nonlinear and alternating, i.e., the values of m_y are positive ($\Delta z < 1.3D$) and negative ($\Delta z > 1.3D$). The region of positive values m_y sets up the prerequisite for the approach of bodies, and the region of negative values, for their drawing apart. The alternating character of the dependence $m_y(\Delta z)$ is mainly determined by the location and intensity of the zones of elevated pressure on the surfaces BS_1 and BS_2. Thus, while with $\Delta z = 1.2D$ diffraction of shock waves significantly contributes to the distribution of local loads, with their drawing apart the effect of this process diminishes. The moment characteristics are in this case more affected by the displacement of the wave structure toward the rear and by the extension of the region of elevated pressure on the body surface BS_1 in the longitudinal direction. The comparison of calculated results and experimental data in Fig. 7 indicates both qualitative and quantitative agreement.

Thus, for a Mach number of the incident flow $M_\infty = 4.03$, the results have been presented of numerical investigations of joint streamlining of two identical axisymmetric bodies at zero angle of attack. The development of the wave structure in the disturbed region and the formation of the regions of elevated pressure on the surface of bodies have been demonstrated by the results of solving the problem for bodies drawn apart ($\Delta z = 1.8D$). The effect of the distance Δz between bodies on disturbed and overall characteristics has been analyzed in the range $\Delta z = 1.2D$–$2D$. It has been shown that, with $\Delta z < 1.3$, a noticeable contribution to the formation of disturbed loads on the body surface and of their moments is made by diffraction of shock waves. With increase in the distance Δz, the basic factor determining total forces and moments is the enlargement of the first region of elevated pressure and its displacement toward the rear of the body. Here, the supersonic interaction of two bodies in the distance range considered involves repulsive forces with an alternating character of the moment. Comparison of calculated results with data of the physical experiment has indicated agreement in both disturbed load and overall aerodynamic characteristics.

The authors express their thanks to A. A. Zheltovodov and I. I. Mazhul' for useful discussion and constant attention to the work.

NOTATION

$C_p = (P - P_\infty)/q_\infty$, dimensionless pressure coefficient; C_z, coefficient of lateral (repulsive) force; D, diameter of the midsection of the frame, m; E, total energy; $f = [\rho, \rho v_x, \rho v_y, \rho v_x, E]^t$, transformed column of conservative variables; $\mathbf{F}(g)$, vector of stream functions; g, gasdynamic parameters; M, Mach number; m_y, coefficient of yaw moment; L, body length, m; $\mathbf{n}(\varphi)$, vector of the external normal to the cylinder surface; P, static pressure, N/m^2; $q_\infty = \rho_\infty W_\infty^2/2$, velocity pressure, N/m^2; $\mathbf{S}$, vector of the area of the cell face; t, time; v_x, v_y, and v_z, components of the vector of the velocity $\mathbf{w}$; W, flow velocity; x_h, head length; β, semivertex angle of a bow wave; $\delta = \arccos[\mathbf{wn}(\varphi)]$, angle between the velocity vector and the normal to the body surface; θ, semivertex angle of the conical head of a body; λ_c, fineness ratio of the cylinder; ρ, density; Ω, cell volume; ω, angle of "encounter" of front shocks; ω_{cr}, critical value of the angle of "encounter". Subscripts and superscripts: h and c, head and cylindrical part of the frame; ∞, parameters of the incident flow; cr, critical; t, transformation.

REFERENCES

1. V. S. Dem'yanenko and E. K. Derunov, Interference of bodies of revolution at hypersonic velocities, in: *Aerophyiscal Studies*, Issue 3, *Gasdynamics and Physical Kinetics* [in Russian], Collection of Sci. Papers, Institute

of Theoretical and Applied Mechanics of the Siberian Branch of the USSR Academy of Sciences, Novosibirsk (1974), pp. 114–116.
2. M. D. Brodetskii and E. K. Derunov, Aerodynamic interference of two bodies of revolution at hypersonic velocities, in: A. M. Kharitonov (Ed.), *Collection of Sci. Papers* [in Russian], Institute of Theoretical and Applied Mechanics of the Siberian Branch of the USSR Academy of Sciences, Novosibirsk (1987), pp. 39–53.
3. Yu. P. Gun'ko and B. Yu. Zanin, Experimental study of interaction of a body of revolution and a wedge with a plane surface, in: *Problems of Aerogasdynamics of Hypersonic Spatial Flows* [in Russian], Collection of Sci. Papers, Institute of Theoretical and Applied Mechanics of the Siberian Branch of the USSR Academy of Sciences, Novosibirsk (1979), pp. 45–57.
4. V. F. Volkov, An Algorithm of Numerical Solution of the Problems of Spatial Hypersonic Interaction of Two Bodies [in Russian], Preprint No. 29-87 of the Institute of Theoretical and Applied Mechanics of the Siberian Branch of the USSR Academy of Sciences, Novosibirsk (1979).
5. M. D. Brodetskii, E. K. Derunov, A. M. Kharitonov, A. V. Zabrodin, and A. E. Lutskii, Comparison of the results of computational and experimental studies of hypersonic flow past a combination of two bodies of revolution above a plane surface, *Teplofiz. Aéromekh.*, **2**, No. 2, 97–102 (1995).
6. M. D. Brodetskii, E. K. Derunov, A. M. Kharitonov, A. V. Zabrodin, and A. E. Lutskii, Interference of combination of bodies in a hypersonic flow past bodies. 1. Streamlining of one body of revolution above a plane surafce, *Teplofiz. Aéromekh.*, **5**, No. 3, 301–306 (1998).
7. M. D. Brodetskii, E. K. Derunov, A. M. Kharitonov, A. V. Zabrodin, and A. E. Lutskii, Interference of combination of bodies in a hypersonic flow past bodies. 2. Streamlining of two bodies of revolution above a plane surafce, *Teplofiz. Aéromekh.*, **6**, No. 2, 165–172 (1999).
8. V. V. Eremin, V. A. Mikhalin, and A. V. Rodionov, Calculation of aerodynamic interference of the elements of rocket carriers at hyperosnic velocities, *Aéromekh. Gaz. Dinam.*, No. 1, 24–35 (2002).
9. V. F. Volkov, E. K. Derunov, A. A. Zheltovodov, and A. I. Maksimov, Verification of numerical computations of supersonic flow around two bodies of revolution in the presence of surface, in: *Proc. Int. Conf. on the Methods of Aerophys. Research.*, 28 June–3 July 2004, Russia, Novosibirsk (2004), Pt. I, pp. 214–221.
10. A. P. Shashkin and V. F. Volkov, A scheme of numerical calculation of inviscid gasdynamic flows, in: *Problems of Flows Past Bodies of Spatial Configurations* [in Russian], Collection of Sci. Papers, Institute of Theoretical and Applied Mechanics of the Siberian Branch of the USSR Academy of Sciences, Novosibirsk (1978), pp. 17–56.
11. V. F. Volkov and I. I. Shabalin, Marching scheme of calculation of two-dimensional hypersonic flows of inviscid gas, *Mat. Modelir.*, **10**, No. 2, 3–14 (1998).
12. G. B. Whitham (A. B. Shabat Ed.), *Linear and Nolinear Waves* [Russian translation], Mir, Moscow (1977).
13. G. A. Arutyunyan and L. V. Karchevskii, *Reflected Shock Waves* [in Russian], Mashinostroenie, Moscow (1973).